ON SELF-APPROACHING AND INCREASING-CHORD DRAWINGS OF 3-CONNECTED PLANAR GRAPHS*

Martin Nöllenburg,† *Roman Prutkin,*‡ *and Ignaz Rutter*‡

Abstract. An *st*-path in a drawing of a graph is *self-approaching* if during the traversal of the corresponding curve from s to any point t' on the curve the distance to t' is non-increasing. A path is *increasing-chord* if it is self-approaching in both directions. A drawing is self-approaching (increasing-chord) if any pair of vertices is connected by a self-approaching (increasing-chord) path.

We study self-approaching and increasing-chord drawings of triangulations and 3-connected planar graphs. We show that in the Euclidean plane, triangulations admit increasing-chord drawings, and for planar 3-trees we can ensure planarity. We prove that strongly monotone (and thus increasing-chord) drawings of trees and binary cactuses require exponential resolution in the worst case, answering an open question by Kindermann et al. [14]. Moreover, we provide a binary cactus that does not admit a self-approaching drawing. Finally, we show that 3-connected planar graphs admit increasing-chord drawings in the hyperbolic plane and characterize the trees that admit such drawings.

1 Introduction

Finding paths between two vertices is one of the most fundamental tasks users want to solve when considering graph drawings [16], for example to find a connection in a schematic map of a public transport system. Empirical studies have shown that users perform better in path-finding tasks if the drawings exhibit a strong geodesic-path tendency [12, 21]. Not surprisingly, graph drawings in which a path with certain properties exists between every pair of vertices have become a popular research topic. Over the last years a number of different drawing conventions implementing the notion of strong geodesic-path tendency have been suggested, namely *greedy drawings* [22], *(strongly) monotone drawings* [2], and *self-approaching* and *increasing-chord drawings* [1]. Note that throughout this paper, all drawings are straight-line and vertices are mapped to distinct points.

The notion of greedy drawings came first and was introduced by Rao et al. [22]. Motivated by greedy routing schemes, e.g., for sensor networks, one seeks a drawing where for every pair of vertices s and t, there exists an *st*-path, along which the distance to t decreases in every vertex. This ensures that greedily sending a message to a vertex that is

*A preliminary version of this paper appeared at the 22nd International Symposium on Graph Drawing, Würzburg, Germany [19]

†*Algorithms and Complexity Group, TU Wien, Vienna, Austria*, noellenburg@ac.tuwien.ac.at

‡*Institute of Theoretical Informatics, Karlsruhe Institute of Technology, Karlsruhe, Germany*, [roman.prutkin|ignaz.rutter]@kit.edu

closer to the destination guarantees delivery. Papadimitriou and Ratajczak conjectured that every 3-connected planar graph admits a greedy embedding into the Euclidean plane [20]. This conjecture has been proved independently by Leighton and Moitra [17] and Angelini et al. [5]. Kleinberg [15] showed that every connected graph has a greedy drawing in the hyperbolic plane. Eppstein and Goodrich [9] showed how to construct such an embedding, in which the coordinates of each vertex are represented using only $O(\log n)$ bits, and Goodrich and Strash [11] provided a corresponding *succinct* representation for greedy embeddings of 3-connected planar graphs in $\mathbb{R}^2$. Angelini et al. [3] showed that some graphs require exponential area for a greedy drawing in $\mathbb{R}^2$. Wang and He [25] used a custom distance metric to construct planar, convex and succinct greedy embeddings of 3-connected planar graphs using Schnyder realizers [24]. Nöllenburg and Prutkin [18] characterized trees admitting a Euclidean greedy embedding. However, a number of interesting questions remain open, e.g., whether every 3-connected planar graph admits a planar and convex Euclidean greedy embedding (strong Papadimitriou-Ratajczak conjecture [20]). Regarding planar greedy drawings of triangulations, the only known result is an existential proof and a heuristic construction by Dhandapani [8] based on face-weighted Schnyder drawings.

While getting closer to the destination in each step, a greedy path can make numerous turns and may even look like a spiral, which hardly matches the intuitive notion of geodesic-path tendency. To overcome this, Angelini et al. [2] introduced monotone drawings, where one requires that for every pair of vertices s and t there exists a *monotone path*, i.e., a path that is monotone with respect to some direction. Ideally, the monotonicity direction should be $\overrightarrow{st}$. This property is called *strong monotonicity*. Angelini et al. showed that biconnected planar graphs admit monotone drawings [2] and that plane graphs admit monotone drawings with few bends [4]. Kindermann et al. [14] showed that every tree admits a strongly monotone drawing. The existence of strongly monotone planar drawings remains open, even for triangulations.

Both greedy and monotone paths may have arbitrarily large *detour*, i.e., the ratio between the path length and the distance of the endpoints can, in general, not be bounded by a constant. Motivated by this fact, Alamdari et al. [1] recently initiated the study of *self-approaching* graph drawings. Self-approaching curves, introduced by Icking [13], are curves, where for any point t' on the curve, the distance to t' is continuously non-increasing while traversing the curve from the start to t'. Equivalently, a curve is self-approaching if, for any three points a, b, c in this order along the curve, it is $\text{dist}(a, c) \geq \text{dist}(b, c)$, where dist() denotes the Euclidean distance. An even stricter requirement are so-called *increasing-chord* curves, which are curves that are self-approaching in both directions. The name is motivated by the characterization of such curves, which states that a curve has increasing chords if and only if for any four distinct points a, b, c, d in that order, it is $\text{dist}(b, c) \leq \text{dist}(a, d)$. Self-approaching curves have detour at most 5.333 [13] and increasing-chord curves have detour at most 2.094 [23]. Alamdari et al. [1] studied the problem of recognizing whether a given graph drawing is self-approaching and gave a complete characterization of trees admitting self-approaching drawings. Furthermore, Alamdari et al. [1] and Frati et al. [7] investigated the problem of connecting given points to obtain an increasing-chord drawing.

We note that every increasing-chord drawing is self-approaching and strongly monotone [1]. The converse is not true. A self-approaching drawing is greedy, but not necessarily

monotone, and a greedy drawing is generally neither self-approaching nor monotone. For trees, the notions of self-approaching and increasing-chord drawing coincide since all paths are unique.

Contribution. We obtain the following results on constructing self-approaching or increasing-chord drawings.

1. We show that every triangulation has an increasing-chord drawing (answering an open question of Alamdari et al. [1]) and construct a *binary cactus* that does not admit a self-approaching drawing (Sect. 3). The latter is a notable difference to greedy drawings since both constructions of greedy drawings for 3-connected planar graphs [5, 17] essentially show that every binary cactus has a greedy drawing. We also prove that strongly monotone (and, thus, increasing-chord) drawings of trees and binary cactuses require exponential resolution in the worst case, answering an open question by Kindermann et al. [14].

2. We show how to construct plane increasing-chord drawings for *planar 3-trees* (a special class of triangulations) using Schnyder realizers (Sect. 4). To the best of our knowledge, this is the first construction for this graph class, even for greedy and strongly monotone plane drawings, which addresses an open question of Angelini et al. [2].

3. We show that, similar to the greedy case [15], the hyperbolic plane $\mathbb{H}^2$ allows representing a broader class of graphs than $\mathbb{R}^2$ (Sect. 5). We prove that a tree has a self-approaching or increasing-chord drawing in $\mathbb{H}^2$ if and only if it either has maximum degree 3 or is a subdivision of $K_{1,4}$ (this is not the case in $\mathbb{R}^2$; see the characterization by Alamdari et al. [1]), implying that every 3-connected planar graph has an increasing-chord drawing. (Barnette proved [6] that 3-connected planar graphs can always be spanned by binary trees.) We also show how to construct planar increasing-chord drawings of binary cactuses in $\mathbb{H}^2$.

2 Preliminaries

For points $a, b, c, d \in \mathbb{R}^2$, let $\mathrm{ray}(a, b)$ denote the ray with origin a and direction $\overrightarrow{ab}$ and let $\mathrm{ray}(a, \overrightarrow{bc})$ denote the ray with origin a and direction $\overrightarrow{bc}$. Let $\mathrm{dir}(ab)$ be the vector $\overrightarrow{ab}$ normalized to unit length. Let $\angle(\overrightarrow{ab}, \overrightarrow{cd})$ denote the smaller angle formed by the two vectors $\overrightarrow{ab}$ and $\overrightarrow{cd}$, and let $\angle abc$ denote the angle $\angle(\overrightarrow{ba}, \overrightarrow{ca})$. For an angle $\alpha \in [0, 2\pi]$, let R_α denote the rotation matrix $\left(\begin{smallmatrix} \cos\alpha & -\sin\alpha \\ \sin\alpha & \cos\alpha \end{smallmatrix}\right)$. For vectors $\overrightarrow{v_1}, \overrightarrow{v_2}$ with $\mathrm{dir}(\overrightarrow{v_2}) = R_\alpha \cdot \mathrm{dir}(\overrightarrow{v_1})$, $\alpha \in [0, 2\pi)$, we write $\angle_{\mathrm{ccw}}(\overrightarrow{v_1}, \overrightarrow{v_2}) := \alpha$.

We reuse some notation from the work of Alamdari et al. [1]. For points $p, q \in \mathbb{R}^2, p \neq q$, let l^+_{pq} denote the halfplane not containing p bounded by the line through q orthogonal to the segment pq. A piecewise-smooth curve is self-approaching if and only if for each point a on the curve, the line perpendicular to the curve at a does not intersect the curve at a later point [13]. This leads to the following characterization of self-approaching paths.

Fact 1 (Corollary 2 in [1]). *Let $\rho = (v_1, v_2, \ldots, v_k)$ be a directed path embedded in $\mathbb{R}^2$ with straight-line segments. Then, ρ is self-approaching if and only if for all $1 \leq i < j \leq k$, the point v_j lies in $l^+_{v_i v_{i+1}}$.*

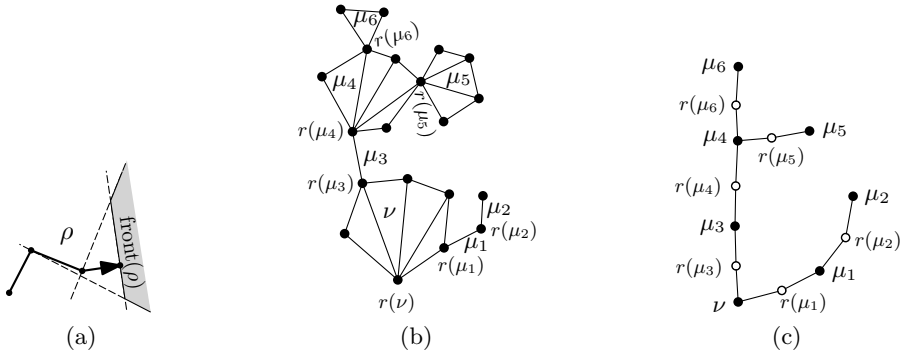

Figure 1: (a) self-approaching path ρ and front(ρ) (gray). (b), (c): downward-triangulated binary cactus and the corresponding BC-tree. B-nodes are black, C-nodes white.

We shall denote the reverse of a path ρ by ρ^{-1}. Let $\rho = (v_1, v_2, \ldots, v_k)$ be a self-approaching path. Define $\text{front}(\rho) = \bigcap_{i=1}^{k-1} l^+_{v_i v_{i+1}}$, see also Fig. 1a. Using Fact 1, we can decide whether a concatenation of two paths is self-approaching.

Fact 2. *Let $\rho_1 = (v_1, \ldots, v_k)$ and $\rho_2 = (v_k, v_{k+1}, \ldots, v_m)$ be self-approaching paths. The path $\rho_1.\rho_2 := (v_1, \ldots, v_k, v_{k+1}, \ldots, v_m)$ is self-approaching if and only if $\rho_2 \subseteq \text{front}(\rho_1)$.*

A path ρ has *increasing chords* if for any points a, b, c, d in this order along ρ, it is $\text{dist}(b, c) \leq \text{dist}(a, d)$. A path has increasing chords if and only if it is self-approaching in both directions. The following result can be obtained as a corollary of Lemma 3 in [13].

Lemma 1. *Let $\rho = (v_1, \ldots, v_k)$ be a path such that for any $i < j$, $i, j \in \{1, \ldots, k-1\}$, it is $\angle(\overrightarrow{v_i v_{i+1}}, \overrightarrow{v_j v_{j+1}}) \leq 90°$. Then, ρ has increasing chords.*

Proof. For any $j > i$, $i, j \in \{1, \ldots, k-1\}$, it is $\angle(\overrightarrow{v_{j+1} v_j}, \overrightarrow{v_{i+1} v_i}) \leq 90°$. Thus, the condition of the lemma also holds for ρ^{-1}, and by symmetry it is sufficient to prove that ρ is self-approaching.

We claim that for each $i \in \{1, \ldots, k-1\}$ and each $j \in \{i+1, \ldots, k\}$, it is $v_j \in l^+_{v_i v_{i+1}}$. Once the claim is proved, it follows from Fact 1 that ρ is self-approaching. For the proof of the claim let $i \in \{1, \ldots, k-1\}$ be arbitrary and fixed. It suffices to show that $v_{i+2}, \ldots, v_k \in l^+_{v_i v_{i+1}}$.

First consider v_{i+2}. By the condition of the lemma, it is $\angle(\overrightarrow{v_i v_{i+1}}, \overrightarrow{v_{i+1} v_{i+2}}) \leq 90°$. Therefore, $v_{i+2} \in l^+_{v_i v_{i+1}}$. Now assume $v_j \in l^+_{v_i v_{i+1}}$ for some $j \in \{i+2, \ldots, k-1\}$. We show $v_{j+1} \in l^+_{v_i v_{i+1}}$. Consider the halfplane $h \subseteq l^+_{v_i v_{i+1}}$ whose boundary is parallel to that of $l^+_{v_i v_{i+1}}$ and contains v_j. Since $\angle(\overrightarrow{v_i v_{i+1}}, \overrightarrow{v_j v_{j+1}}) \leq 90°$, it is $v_{j+1} \in h \subseteq l^+_{v_i v_{i+1}}$. □

Let $G = (V, E)$ be a connected graph. A *separating k-set* is a set of k vertices whose removal disconnects the graph. A vertex forming a separating 1-set is called *cutvertex*. A graph is *c-connected* if it does not admit a separating k-set with $k \leq c - 1$; 2-connected graphs are also called *biconnected*. A connected graph is biconnected if and only if it does not contain a cutvertex. A *block* is a maximal biconnected subgraph. The *block-cutvertex*

tree (or *BC-tree*) T_G of G has a *B-node* for each block of G, a *C-node* for each cutvertex of G and, for each block ν containing a cutvertex v, an edge between the corresponding B- and C-node. We associate B-nodes with their corresponding blocks and C-nodes with their corresponding cutvertices.

The following notation follows the work of Angelini et al. [5]. Let T_G be rooted at some block ν containing a non-cutvertex (such a block ν always exists). For each block $\mu \neq \nu$, let $\pi(\mu)$ denote the *parent block* of μ, i.e., the grandparent of μ in T_G. Let $\pi^2(\mu)$ denote the parent block of $\pi(\mu)$ and, generally, $\pi^{i+1}(\mu)$ the parent block of $\pi^i(\mu)$. Further, we define the *root* $r(\mu)$ of μ as the cutvertex contained in both μ and $\pi(\mu)$. Note that $r(\mu)$ is the parent of μ in T_G. In addition, for the root node ν of T_G, we define $r(\nu)$ to be some non-cutvertex of ν. Let $\mathrm{depth}_B(\mu)$ denote the number of B-nodes on the $\nu\mu$-path in T_G minus 1, and let $\mathrm{depth}_C(r(\mu)) = \mathrm{depth}_B(\mu)$. If μ is a leaf of T_G, we call it a *leaf block*.

A *cactus* is a graph in which every edge is part of at most one cycle. Note that every cactus is outerplanar. In a *binary* cactus every cutvertex is part of exactly two blocks. For a binary cactus G with a block μ containing a cutvertex v, let G^v_μ denote the maximal connected subgraph containing v but no other vertex of μ. We say that G^v_μ is a *subcactus* of G. Let G be a binary cactus with a fixed root and let v be a cutvertex of G. Then the block μ containing v such that $v \neq r(\mu)$ is unique, and we write G^v for G^v_μ.

A *triangulated* cactus is a cactus together with additional edges, which make each of the cactus blocks internally triangulated. A *triangular fan with vertices* $V_t = \{v_0, v_1, \ldots, v_k\}$ *and root* v_0 is a graph on V_t with edges v_iv_{i+1}, $i = 1, \ldots, k-1$, as well as v_0v_i, $i = 1, \ldots, k$. Let us consider a special kind of triangulated cactuses, each of whose blocks μ is a triangular fan with root $r(\mu)$. We call such a cactus *downward-triangulated* and every edge of a block μ incident to $r(\mu)$ a *downward* edge. Fig. 1b and 1c show a downward-triangulated binary cactus and the corresponding BC-tree.

Consider a fixed straight-line drawing of a cactus G with root r. We define the set of *upward directed* edges $E_U(G) = \{r(\mu)v \mid \mu \text{ is a block of } G \text{ containing } v,\ v \neq r(\mu)\}$. Note that if G is not triangulated, some edges in $E_U(G)$ might not be edges in G. We define the set of *upward* directions $U(G) = \{\overrightarrow{r(\mu)v} \mid \mu \text{ is a block of } G \text{ containing } v,\ v \neq r(\mu)\}$ and the set of *downward* directions $D(G) = \{\overrightarrow{uv} \mid \overrightarrow{vu} \in U(G)\}$. If G is binary, then, for cutvertex u, let U_u denote the upward directed edges of the subcactus rooted at u or, formally, $U_u = E_U(G^u)$.

3 Graphs with Self-Approaching Drawings

A natural approach to construct (not necessarily plane) self-approaching drawings is to construct a self-approaching drawing of a spanning subgraph. For instance, to draw a graph G containing a Hamiltonian path H with increasing chords, we simply draw H consecutively on a line. In this section, we consider 3-connected planar graphs and the special case of triangulations, which addresses an open question of Alamdari et al. [1]. These graphs are known to have a spanning binary cactus [5, 17]. Angelini et al. [5] showed that every triangulation has a spanning downward-triangulated binary cactus.

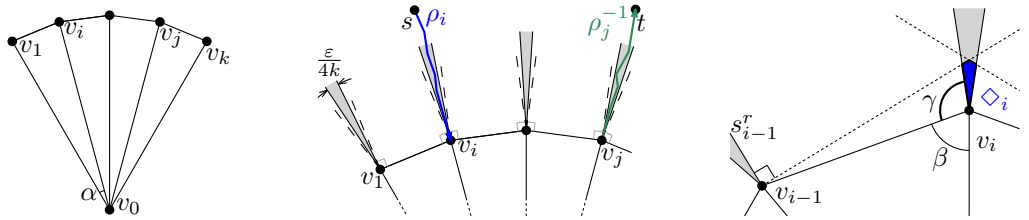

Figure 2: Drawing a triangulated binary cactus with increasing chords inductively. The drawings $\Gamma_{i,\varepsilon'}$ of the subcactuses, $\varepsilon' = \frac{\varepsilon}{4k}$, are contained inside the gray cones. It is $\beta = 90° - \varepsilon'$, $\gamma = 90° + \varepsilon'/2$.

3.1 Increasing-chord drawings of triangulations

We show that every downward-triangulated binary cactus has an increasing-chord drawing. The construction is similar to the one of the greedy drawings of binary cactuses in the two proofs of the Papadimitriou-Ratajczak conjecture [5, 17]. Our proof is by induction on the height of the BC-tree. We show that G can be drawn such that all downward edges are almost vertical and the remaining edges almost horizontal. Then, for vertices s, t of G, an st-path with increasing chords goes downwards to some block μ, then sideways to another cutvertex of μ and, finally, upwards to t. Let $\vec{e_1}, \vec{e_2}$ be vectors $(1,0)^\top$, $(0,1)^\top$ respectively.

Theorem 1. *Let $G = (V, E)$ be a downward-triangulated binary cactus. For any $0° < \varepsilon < 90°$, there exists an increasing-chord drawing Γ_ε of G, such that for each vertex v contained in some block μ, $v \neq r(\mu)$, the angle formed by $\overrightarrow{r(\mu)v}$ and $\vec{e_2}$ is less than $\frac{\varepsilon}{2}$.*

Proof. Let G be rooted at block ν. As our base case, let $\nu = G$ be a triangular fan with vertices $v_0, v_1, \ldots, v_k$ and root $v_0 = r(\nu)$. We draw v_0 at the origin and distribute $v_1, \ldots, v_k$ on the unit circle, such that $\angle(\vec{e_2}, \overrightarrow{v_0v_1}) = k\alpha/2$ and $\angle(\overrightarrow{v_0v_i}, \overrightarrow{v_0v_{i+1}}) = \alpha$, $\alpha = \varepsilon/2k$; see Fig. 2a. By Lemma 1, path $(v_1, \ldots, v_k)$ has increasing chords.

Now let G have multiple blocks. We draw the root block ν, $v_0 = r(\nu)$, as in the previous case, but with $\alpha = \frac{\varepsilon}{2k}$. Then, for each $i = 1, \ldots, k$, we choose $\varepsilon' = \frac{\varepsilon}{4k}$ and draw the subcactus $G_i = G_\nu^{v_i}$ rooted at v_i inductively, such that the corresponding drawing $\Gamma_{i,\varepsilon'}$ is aligned at $\overrightarrow{v_0v_i}$ instead of $\vec{e_2}$; see Fig 2b. Note that ε' is the angle of the cones (gray) containing $\Gamma_{i,\varepsilon'}$. Obviously, all downward edges of G form angles less than $\frac{\varepsilon}{2}$ with $\vec{e_2}$.

We must be able to reach any t in any G_j from any s in any G_i via an increasing-chord path ρ. To achieve this, we make sure that no normal on a downward edge of G_i crosses the drawing of G_j, $j \neq i$. Let Λ_i be the cone with apex v_i and angle ε' aligned with $\overrightarrow{v_0v_i}$, $v_0 \notin \Lambda_i$ (gray regions in Fig. 2b). Let s_i^l and s_i^r be the left and right boundary rays of Λ_i with respect to the direction of $\overrightarrow{v_0v_i}$, and h_i^l, h_i^r the halfplanes with boundaries containing v_i and orthogonal to s_i^l and s_i^r respectively, such that $v_0 \in h_i^l \cap h_i^r$. For $i = 2, \ldots, k-1$, define $\Diamond_i = \Lambda_i \cap h_{i-1}^r \cap h_{i+1}^l$ (thin blue quadrilateral in Fig. 2c). Let $\Diamond_1 = \Lambda_1 \cap h_2^l$ and $\Diamond_k = \Lambda_k \cap h_{k-1}^r$. For any $i, j = 1, \ldots, k$, $i \neq j$, it holds $\Diamond_j \subseteq h_i^r \cap h_i^l$. We now scale each drawing $\Gamma_{i,\varepsilon'}$ such that it is contained in $\Diamond_i$. In particular, for any downward edge uv in $\Gamma_{i,\varepsilon'}$, we have $\Gamma_{j,\varepsilon'} \subseteq \Diamond_j \subseteq l_{uv}^+$ for $j \neq i$. We claim that the resulting drawing of G is an increasing-chord

drawing.

Consider vertices s,t of G. If s and t are contained in the same subgraph G_i, an increasing-chord st-path in G_i exists by induction. If s is in G_i and t is v_0, let ρ_i be the sv_i-path in G_i that uses only downward edges. By Lemma 1, path ρ_i is increasing-chord and remains so after adding edge v_iv_0.

Finally, assume t is in G_j with $j \neq i$. Let ρ_j be the tv_j-path in G_j that uses only downward edges. Due to the choice of ε', $h_i^r \cap h_i^l \subseteq \text{front}(\rho_i)$ contains $v_1, \ldots, v_k$ in its interior. Consider the path $\rho' = (v_i, v_{i+1}, \ldots, v_j)$. It is self-approaching by Lemma 1; also, $\rho' \subseteq \text{front}(\rho_i)$ and $\rho_j \subseteq \text{front}(\rho')$. It also holds $\rho_j \subseteq \Diamond_j \subseteq \text{front}(\rho_i)$. Fact 2 lets us concatenate ρ_i, ρ' and ρ_j^{-1} to a self-approaching path. By a symmetric argument, it is also self-approaching in the opposite direction and, thus, is increasing-chord. □

Since every triangulation has a spanning downward-triangulated binary cactus [5], this implies that planar triangulations admit increasing-chord drawings.

Corollary 1. *Every planar triangulation admits an increasing-chord drawing.*

3.2 Exponential worst case resolution

The construction for a spanning downward-triangulated binary cactus in Section 3.1 requires exponential area. In this section, we show that we cannot do better in the worst case even for strongly monotone drawings of downward-triangulated binary cactuses. Recall that increasing-chord drawings are strongly monotone.

For the following lemma, we want to point out the difference between a *greedy st-path* and a *greedy drawing* of a graph G, such that G is a path. In a fixed drawing, a st-path $\rho = (v_0 = s, v_1, \ldots, v_k, v_{k+1} = t)$ is greedy (or *distance-decreasing*), if it is $|v_{i+1}t| < |v_it|$ for every $i = 0, \ldots, k$. Note that for some $0 \leq i < j \leq k+1$, $\{i, j\} \neq \{0, k+1\}$, the v_iv_j-path $(v_i, v_{i+1}, \ldots, v_j)$ is not necessarily greedy; see Fig. 3a. On the other hand, for a graph G which is a path $\rho = (v_0, v_1, \ldots, v_k, v_{k+1})$, a drawing Γ is a greedy drawing of G if every v_iv_j-path $(v_i, v_{i+1}, \ldots, v_j)$ and every v_jv_i-path $(v_j, v_{j-1}, \ldots, v_i)$ in Γ is a greedy path for any $0 \leq i < j \leq k+1$.

The following lemma describes directions of certain edges in a greedy or monotone drawing of a cactus.

Lemma 2. *For a cactus $G = (V, E)$ and two vertices $s, t \in V$, consider the cutvertices v_1, …, v_k lying on every st-path in G in this order. In any greedy drawing of G, connecting consecutive vertices in $(s, v_1, \ldots, v_k, t)$ would form a greedy drawing of the path $(s, v_1, \ldots, v_k, t)$. In any monotone drawing, connecting consecutive vertices in $(s, v_1, \ldots, v_k, t)$ would form a monotone drawing of the path $(s, v_1, \ldots, v_k, t)$. In both cases, $\text{ray}(v_1, s)$ and $\text{ray}(v_k, t)$ diverge.*

Proof. Let $v_0 = s$, $v_{k+1} = t$. For $0 \leq i < j \leq k+1$, any v_iv_j-path and any v_jv_i-path in G contains vertices v_i, v_{i+1}, …, v_j. Since a path in a greedy drawing of G remains greedy after

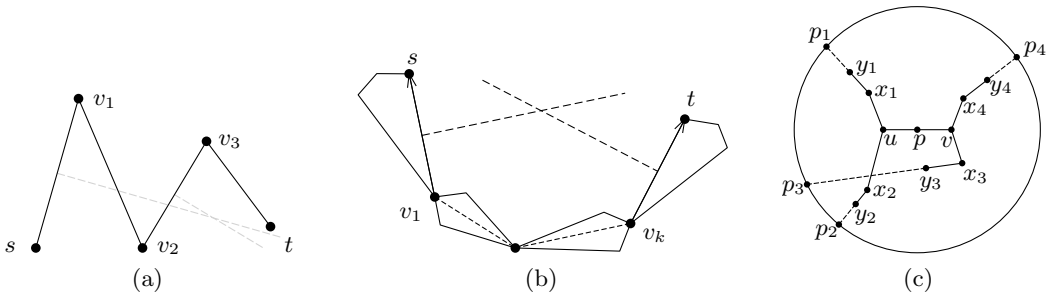

Figure 3: (a) The st-path (s, v_1, v_2, v_3, t) is a greedy path, but its sv_2 subpath is not. Thus, this drawing is not a greedy drawing of a path. (b) Proof of Lemma 2. (c) Proof of Lemma 3.

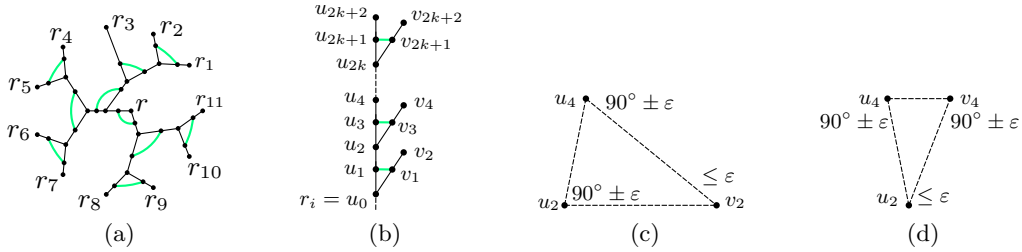

Figure 4: Family of binary cactuses G_k requiring exponential area for any strongly monotone drawing. (a) Central cactus G'; (b) binary subcactus C_k attached to each vertex of degree 1 of G'. In a strongly monotone drawing of G_k, it must hold: (c) $|u_2u_4| \leq |u_2v_2| \tan\varepsilon$; (d) $|u_4v_4| \leq |u_2u_4| \tan\varepsilon$.

replacing subpaths by shortcuts, the segments sv_1, v_1v_2, …, $v_{k-1}v_k$, v_kv_t form a greedy drawing. By Lemma 7 of Angelini et al. [3], $\mathrm{ray}(v_1, s)$ and $\mathrm{ray}(v_k, t)$ diverge; see Fig. 3b.

Analogously, a path remains monotone after replacing subpaths by shortcuts. Therefore, in a monotone drawing of G, segments sv_1, v_1v_2, …, $v_{k-1}v_k$, v_kv_t form a monotone drawing. Since a monotone path cannot make a turn of 180° or more, $\mathrm{ray}(v_1, s)$ and $\mathrm{ray}(v_k, t)$ must diverge. □

For the following lemma, consider a greedy or monotone drawing of a cactus G with root r. Recall that for a cutvertex u, the set U_u denotes the upward directed edges of the subcactus rooted at u, or, formally, $U_u = E_U(G^u)$. Then, the following property holds.

Lemma 3. *In a monotone or greedy drawing of a cactus with root r, consider cutvertices $u, v \neq r$, such that the subcactuses G^u and G^v are disjoint. Then the edges in U_u and in U_v each form a single interval in the circular order induced by their joint set of directions.*

Proof. Consider four pairs of vertices x_i, y_i, $i = 1, \ldots, 4$, such that $x_iy_i \in U_u$ for $i = 1, 2$ and $x_iy_i \in U_v$ for $i = 3, 4$. Note that, by the definition of U_u and U_v, vertices x_i and x_j are cutvertices. For $i = 1, 2$, $j = 3, 4$, let ρ_{ij} denote the vertex sequence y_i, x_i, u, v, x_j, y_j. Since x_i, u, v, x_j are cutvertices, ρ_{ij} is a subsequence of every y_iy_j-path. By Lemma 2, each such ρ_{ij} forms a monotone or a greedy drawing of a path, respectively. Hence, ρ_{ij} is non-crossing and cannot make a turn of 180° or more. Additionally, by Lemma 2, rays

ray(x_i, y_i) and ray(x_j, y_j) must diverge. Finally, ray(x_j, y_j) cannot cross ρ_{ij}, since this would imply that ρ_{ij} has made a turn of 180° or more, and neither can ray(x_i, y_i).

We define $p = (u + v)/2$ and choose an arbitrary $R > 0$, such that all paths ρ_{ij} are contained inside a circle C with center p and radius R. Let p_i be the intersection of ray(x_i, y_i) and C. Assume p_1, p_3, p_2, p_4 is the counterclockwise order of p_i on the boundary of C; see Fig. 3c. Then, for some pair i, j, $i \in \{1, 2\}$, $j \in \{3, 4\}$, there exists a crossing of ray(x_i, y_i) or ray(x_j, y_j) with ρ_{ij} or with each other; a contradiction. Therefore, p_1, p_2 as well as p_3, p_4 appear consecutively on the boundary of C. Now let the radius R approach infinity. Then, $\overrightarrow{pp_i}$ becomes parallel with $\overrightarrow{x_i y_i}$. Therefore, the circular order $\overrightarrow{x_1y_1}$, $\overrightarrow{x_3y_3}$, $\overrightarrow{x_2y_2}$, $\overrightarrow{x_4y_4}$ is not possible, and the statement follows. □

Note that for trees, Angelini et al. [2] call this property *slope disjointness*. Consider the following family of binary cactuses G_k. Let G' be a rooted binary cactus with eleven vertices $r_1, \ldots, r_{11}$ of degree 1 and its root r as the only vertex of degree 2; see Fig. 4a. Next, consider cactus C_k consisting of a chain of $k + 1$ triangles and some additional degree-1 nodes as in Fig. 4b. We construct G_k by attaching a copy of C_k to each r_i in G'. From now on, consider a strongly monotone drawing of G_k.

Using Lemma 3 and the pigeonhole principle, we can show the following fact.

Lemma 4. *For some r_i, $i \in \{1, \ldots, 11\}$, each pair of directions in U_{r_i} forms an angle at most $\varepsilon = 360°/11$.*

Proof. Consider the two cutvertices of the root block of G_k; see Fig. 4a. By Lemma 3, vectors in $U_{r_1} \cup \cdots \cup U_{r_{11}}$ appear in the following circular order: first the vectors in $U_{r_1} \cup \cdots \cup U_{r_7}$, then the vectors in $U_{r_8} \cup \cdots \cup U_{r_{11}}$. By applying the same argument to the child blocks repetitively, it follows that the vectors have the following circular order: first the vectors in $U_{r_{\pi(1)}}$, then the vectors in $U_{r_{\pi(2)}}$, …, then the vectors in $U_{r_{\pi(11)}}$ for some permutation π. Therefore, for some i, each pair of directions in U_{r_i} forms an angle at most $\varepsilon = 360°/11$. □

Now consider a vertex r_i with the property of Lemma 4. Let the vertices of its subcactus be named as in Fig. 4b. Without loss of generality, we may assume that each vector in U_{r_i} forms an angle at most $\varepsilon/2$ with the upward direction $\vec{e_2}$. We show that certain directions have to be almost horizontal.

Lemma 5. *For even i, j, $2 \le j \le i \le 2k + 2$, consider vertices u_i, v_j. Vector $\overrightarrow{u_i v_j}$ forms an angle at most $\varepsilon/2$ with the horizontal axis.*

Proof. Consider a strongly monotone $u_i v_j$-path ρ. Vertices u_i, u_{i-1}, v_{j-1}, v_j must appear on ρ in this order. It is $\angle(\overrightarrow{u_{i-1}u_i}, \overrightarrow{v_{j-1}v_j}) \le \varepsilon$. Furthermore, by the strong monotonicity of ρ, it is $\angle u_{i-1}u_iv_j$, $\angle u_{i-1}v_ju_i < 90°$, as well as $\angle v_{j-1}u_iv_j$, $\angle v_{j-1}v_ju_i < 90°$.

Consider the strip $S = \mathbb{R}^2 \setminus (l^+_{u_iv_j} \cup l^+_{v_ju_i})$; see Fig, 5a. From the above observation on the angles, it follows $u_{i-1}, v_{j-1} \in S$. Line segment u_iv_j divides S into two parts. Assume u_{i-1} and v_{j-1} are in different parts. But then, the angle $\angle(\overrightarrow{u_{i-1}u_i}, \overrightarrow{v_{j-1}v_j})$ is at least 90°, a contradiction. Thus, u_{i-1} and v_{j-1} are in the same part, and, since $\overrightarrow{u_{i-1}u_i}$, $\overrightarrow{v_{j-1}v_j}$ point upwards, vertices u_{i-1} and v_{j-1} are below the line through the segment u_iv_j.

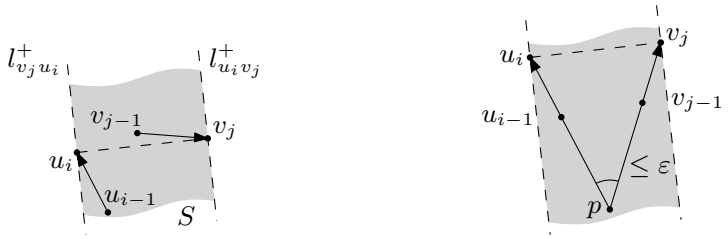

Figure 5: Proof of Lemma 5. (a) Points u_{i-1} and v_{j-1} must lie below $u_i v_j$ inside the strip S. (b) From the triangle $u_i v_j p$, it follows that $\angle p v_j u_i = \angle v_{j-1} v_j u_i < 90°$.

Let p be the intersection of the lines through $u_{i-1}u_i$ and $v_{j-1}v_j$; see Fig. 5b. Point p also lies below the line through $u_i v_j$. Consider the triangle with corners u_i, v_j and p. It is $\angle u_i p v_j = \angle(\overrightarrow{u_{i-1}u_i}, \overrightarrow{v_{j-1}v_j}) \leq \varepsilon$. Furthermore, it is $\angle p u_i v_j = \angle u_{i-1} u_i v_j < 90°$, and $\angle p v_j u_i = \angle v_{j-1} v_j u_i < 90°$. Therefore, $\angle u_{i-1} u_i v_j$, $\angle v_{j-1} v_j u_i \in (90° - \varepsilon, 90°)$.

Assume it is $\angle(\overrightarrow{u_i v_j}, \vec{e_1}) > \varepsilon/2$, and let $\overrightarrow{u_i v_j}$ point upwards and to the right. The other cases are analogous. Then, since $\angle u_{i-1} u_i v_j \in (90° - \varepsilon, 90°)$, edge $u_{u-i} u_i$ must point upwards and to the left, and it must be $\angle(\overrightarrow{u_{i-1}u_i}, \vec{e_2}) > \varepsilon/2$, a contradiction to the above assumption on the directions of the upward edges. Therefore, the statement follows. □

The following lemma essentially shows that G_k requires exponential resolution.

Lemma 6. *For $i = 2, 4, \ldots, 2k$, it holds $|u_{i+2}v_{i+2}| \leq (\tan\varepsilon)^2 |u_i v_i|$.*

Proof. For brevity, let $i = 2$. First, we show that $|u_2 v_2|$ is significantly larger than $|u_2 u_4|$; see Fig. 4c. By Lemma 5, it is $\angle u_2 u_4 v_2 \in (90° - \varepsilon, 90° + \varepsilon)$. Therefore, $\sin\angle u_2 v_2 u_4 \geq \sin(90° - \varepsilon)$. It holds:

$$\frac{|u_2 u_4|}{|u_2 v_2|} = \frac{\sin\angle u_2 v_2 u_4}{\sin\angle u_2 u_4 v_2} \leq \frac{\sin\varepsilon}{\sin(90° - \varepsilon)} = \tan\varepsilon.$$

Next, we show that $|u_2 u_4|$ is significantly larger than $|u_4 v_4|$; see Fig. 4d. By Lemma 5, it is $\angle u_2 v_4 u_4 \in (90° - \varepsilon, 90° + \varepsilon)$. Therefore, $\sin\angle u_2 v_4 u_4 \geq \sin(90° - \varepsilon)$. It holds:

$$\frac{|u_4 v_4|}{|u_2 u_4|} = \frac{\sin\angle u_4 u_2 v_4}{\sin\angle u_2 v_4 u_4} \leq \frac{\sin\varepsilon}{\sin(90° - \varepsilon)} = \tan\varepsilon.$$

Thus, $|u_4 v_4| \leq |u_2 u_4| \tan\varepsilon \leq |u_2 v_2| (\tan\varepsilon)^2$. □

As a consequence of Lemma 6 we get $|u_{2k+2} v_{2k+2}| \leq |u_2 v_2| (\tan\varepsilon)^{2k}$. It is $(\tan\varepsilon)^2 < 0.414$. Since cactus G_k contains $n = \Theta(1) + 44k$ vertices, the following exponential lower bound holds for the resolution of strongly monotone drawings.

Theorem 2. *There exists an infinite family of binary cactuses with n vertices that require resolution $\Omega(2^{\frac{n}{44}})$ for any strongly monotone drawing.*

Using this result, we can construct a family of trees requiring exponential area for any strongly monotone drawing. Consider the binary spanning tree T_k of G_k created by removing the thick green edges in Fig. 4a and 4b. Obviously, by Theorem 2 it requires resolution $\Omega(2^{\frac{n}{44}})$ for any strongly monotone drawing. This answers an open question by Kindermann et al. [14]. Replacing degree-2 vertices by shortcuts and applying a more careful analysis lets us prove the following result.

Theorem 3. *There exists an infinite family of binary trees with n vertices that require resolution $\Omega(2^{\frac{n}{22}})$ for any strongly monotone drawing.*

Observe that exponential worst-case resolution of strongly monotone drawings of binary cactuses is a stronger result than the corresponding statement for trees. A strongly monotone drawing of a binary cactus does not necessarily induce a strongly monotone drawing of any of its spanning trees.

3.3 Non-triangulated cactuses

The construction for an increasing-chord drawing from Section 3.1 fails if the blocks are not triangular fans since we now cannot just use downward edges to reach the common ancestor block. Consider the family of rooted binary cactuses $G_n = (V_n, E_n)$ defined as follows. Graph G_0 is a single 4-cycle, where an arbitrary vertex is designated as the root. For $n \geq 1$, consider two disjoint copies of G_{n-1} with roots a_0 and c_0. We create G_n by adding new vertices r_0 and b_0 both adjacent to a_0 and c_0; see Fig. 6a. For the new block ν containing r_0, a_0, b_0, c_0, we set $r(\nu) = r_0$. We select r_0 as the root of G_n and ν as its root block. For a block μ_i with root r_i, let a_i, b_i, c_i be its remaining vertices, such that $b_i r_i \notin E_n$. For a given drawing, due to the symmetry of G_n, we can rename the vertices a_i and c_i such that $\angle_{\text{ccw}}(\overrightarrow{r_i c_i}, \overrightarrow{r_i a_i}) \leq 180°$. If a fixed block μ_i is considered, we refer to a_i, b_i, c_i as a, b, c for brevity. We now prove the following negative result.

Theorem 4. *For $n \geq 10$, G_n has no self-approaching drawing.*

The outline of the proof is as follows. We show that every self-approaching drawing Γ of G_{10} contains a self-approaching drawing of G_3 such that for each block μ of this G_3, the angle at $r = r(\mu)$ is very small, angles at a and c are 90° or slightly larger (Lemma 8) and such that sides ra and rc have almost the same length which is significantly greater than $\text{dist}(a, c)$ (Lemma 10). In addition, the following properties hold for this G_3.

1. If μ_i is contained in the subcactus rooted at c_j, each self-approaching $b_i a_j$-path uses edge $b_i a_i$, and analogously for the symmetric case; see Lemma 9.

2. Each block is drawn significantly smaller than its parent block; see Lemma 11(i).

3. If the descendants of block μ form subcactuses G_k with $k \geq 2$ on both sides, the parent block of μ must be drawn smaller than μ; see Lemma 11(ii).

Obviously, the second and third conditions are contradictory. Note that every block has to be self-approaching. However, it might be non-convex and even non-planar.

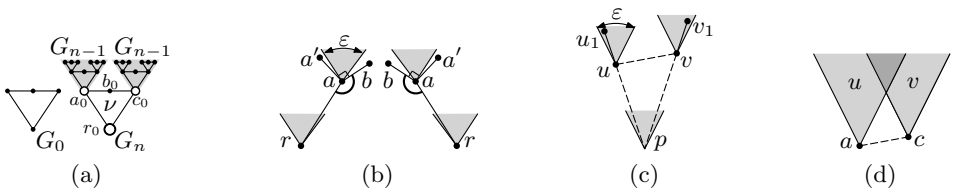

Figure 6: (a) cactuses G_n; (b) Lemma 8(iii); (c),(d): Lemma 8(iv).

Observation 1. *In a self-approaching drawing of a polygon P, no two non-consecutive angles can be both less than $90°$.*

Proof. If P is a triangle, it is trivially self-approaching. Let now v_1, v_2, v_3, v_4 be pairwise distinct vertices appearing in this circular order around the boundary of P. Let the angles at both v_2 and v_4 be less than $90°$. However, a self-approaching v_1v_3-path must use either v_2 or v_4, a contradiction. □

The following lemmas will be used to show that the drawings of certain blocks must be relatively thin, i.e., their downward edges have similar directions.

Lemma 7. *Every self-approaching drawing of G_{10} contains a cutvertex $\bar{r}$, such that each pair of directions in $U_{\bar{r}}$ form an angle at most $\varepsilon = 22.5°$.*

Proof. Denote by r_j, $j = 1, \ldots, 16$, the cutvertices with $\text{depth}_C(r_j) = 4$. By an argument similar to the one in the proof of Lemma 4, the edges in U_{r_j} appear in the following circular order by their directions: first the edges in $U_{r_{\pi(1)}}$, then the edges in $U_{r_{\pi(2)}}$, …, then the edges in $U_{r_{\pi(16)}}$ for some permutation π. Therefore, by the pigeonhole principle, the statement holds for some $j \in \{1, \ldots, 16\}$ and $\bar{r} = r_j$. □

Let $\bar{r}$ be a cutvertex in the fixed drawing at $\text{depth}_C(\bar{r}) = 4$ with the property shown in Lemma 7. Then, $G^{\bar{r}}$ is isomorphic to G_6. From now on, we only consider non-leaf blocks μ_i and vertices r_i, a_i, b_i, c_i in $G^{\bar{r}}$. We shall sometimes name the points a instead of a_i etc. for convenience. We assume $\angle(\vec{e_2}, \vec{ra}), \angle(\vec{e_2}, \vec{rc}) \leq \varepsilon/2$. The following lemma is proved using basic trigonometric arguments.

Lemma 8. *It holds:*

(i) $\angle abc \geq 90°$;

(ii) $G^a \subseteq l^+_{ba}$, $G^c \subseteq l^+_{bc}$;

(iii) $\angle bar \leq 90° + \varepsilon$, $\angle bcr \leq 90° + \varepsilon$.

(iv) *For vertices u in G^a, v in G^c of degree 4 it is $\angle(\vec{uv}, \vec{e_1}) \leq \varepsilon/2$.*

Proof. (i) It is $\angle arc \leq \varepsilon$. Thus, by Observation 1, $\angle abc \geq 90°$.

(ii) Let t be a vertex of G^c. Since $\angle arc \leq \varepsilon < 90°$, any self-approaching at-path must contain bc. Thus, $t \in l^+_{bc}$, and the claim for G^c and, similarly, for G^a follows.

(iii) Consider block μ' containing $a' \neq a$, $r(\mu') = a$; see Fig. 6b. Then, $\angle(\overrightarrow{ra}, \overrightarrow{aa'}) \leq \varepsilon$. By (ii), it is $baa' \geq 90°$. If $\angle bar > 90° + \varepsilon$, it is $\angle(\overrightarrow{ra}, \overrightarrow{aa'}) > \varepsilon$, a contradiction. The same argument applies for $\angle bcr$.

(iv) Since u, v have degree 4, they are roots of some blocks. Let u_1 be a neighbor of u in G^u and v_1 a neighbor of v in G^v maximizing $\angle u_1uv$ and $\angle v_1vu$; see Fig. 6c. By considering self-approaching u_1v and v_1u-paths, it follows $\angle u_1uv, \angle v_1vu \geq 90°$. Also, $\text{ray}(u_1, u)$ and $\text{ray}(v_1, v)$ converge by Lemma 2. Let p be their intersection. Then, $\angle upv \leq \varepsilon$ and $\angle puv, \angle pvu \leq 90°$. It is $\angle(\overrightarrow{pu}, \overrightarrow{e_2}) \leq \varepsilon/2$ and $\angle(\overrightarrow{pv}, \overrightarrow{e_2}) \leq \varepsilon/2$. Therefore, if $\overrightarrow{uv}$ points upward, it forms an angle at most $\varepsilon/2$ with the horizontal direction. If $\overrightarrow{uv}$ points downward, by symmetric arguments, $\overrightarrow{vu}$ forms an angle at most $\varepsilon/2$ with the horizontal direction. The same holds for $\overrightarrow{ac}$, $\overrightarrow{av}$, $\overrightarrow{uc}$.

It remains to show that u is "to the left" of v. Since it is $\angle_{\text{ccw}}(\overrightarrow{rc}, \overrightarrow{ra}) < 180°$ and $\angle(\overrightarrow{rc}, \overrightarrow{ra}) \leq \varepsilon$, it is $\angle(\overrightarrow{ac}, \overrightarrow{e_1}) \leq \varepsilon/2$. Consider the two vertically aligned cones with apices a and c and angle ε (gray in Fig. 6d). Vertex u must be in the cone of a, and vertex v in the cone of c. If u is not in the cone of c and, at the same time, v not in the cone of a, then v is to the right of u. In this case, it is $\angle(\overrightarrow{uv}, \overrightarrow{e_1}) \leq \varepsilon/2$, and we are done.

Now assume $\angle(\overrightarrow{uv}, -\overrightarrow{e_1}) \leq \varepsilon/2$. Then, by the above argument, u is in the cone of c or v in the cone of a (without loss of generality, u is in the cone of a). Thus, u must be in the dark gray area in Fig. 6d). This contradicts the fact that $\overrightarrow{uc}$ forms an angle of at most $\varepsilon/2$ with the horizontal direction. □

We can now describe block angles at a_i, c_i more precisely and characterize certain self-approaching paths in $G^{\bar{r}}$. We show that a self-approaching path from b_i *downwards and to the left*, i.e., to an ancestor block μ_j of μ_i, such that μ_i is in G^{c_j}, must use a_i. Similarly, a self-approaching path *downwards and to the right* must use c_i. Since for several ancestor blocks of μ_i the roots lie on both of these two kinds of paths, we can bound the area containing them and show that it is relatively small. This implies that the ancestor blocks are small as well, providing a contradiction.

Lemma 9. *Consider non-leaf blocks μ_0, μ_1, μ_2, such that $r(\mu_1) = c_0$ and μ_2 in G^{a_1}; see Fig. 7a.*

(i) *It is $\angle r_2a_2b_2, \angle r_2c_2b_2 \in [90°, 90° + \varepsilon]$, b_2 lies to the right of* $\text{ray}(r_2, a_2)$ *and to the left of* $\text{ray}(r_2, c_2)$.

(ii) *Each self-approaching b_2a_0-path uses a_2; each self-approaching b_2c_1-path uses c_2.*

Proof. (i) Assume $\angle r_2a_2b_2 < 90°$. Then, all self-approaching b_2a_0 and b_2c_1-paths must use c_2. By Lemma 8(iv), the lines through a_0c_2 and c_2c_1 are "almost horizontal", i.e., $\angle(\overrightarrow{a_0c_2}, \overrightarrow{e_1}), \angle(\overrightarrow{c_2c_1}, \overrightarrow{e_1}) \leq \varepsilon/2$. Since r_2c_2 is "almost vertical", r_2 must lie below these lines and it is $\angle a_0c_2r_2, \angle c_1c_2r_2 \in [90° - \varepsilon, 90° + \varepsilon]$; see Fig. 7b.

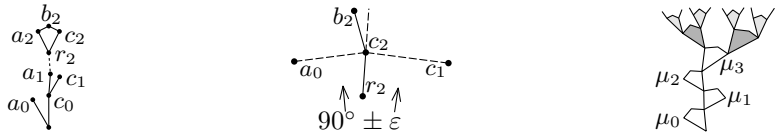

Figure 7: (a),(b) construction for Lemma 9; (c) subcactus G_6 providing the contradiction in the proof of Theorem 4.

First, let b_2 lie to the left of $\text{ray}(r_2, c_2)$. Recall that by our assumption it is $\angle r_2c_2b_2 \geq 90°$. Furthermore, since every self-approaching b_2a_0-path must use c_2, it is $\angle a_0c_2b_2 \geq 90°$. Therefore, b_2 cannot lie inside the counterclockwise angle between c_2a_0 and c_2r_2, since it is $\angle_{\text{ccw}}(\overrightarrow{c_2a_0}, \overrightarrow{c_2r_2}) \leq 90° + \varepsilon < \angle r_2c_2b_2 + \angle a_0c_2b_2$. Thus, b_2 is above a_0c_2, and it is $\angle r_2c_2b_2 = \angle a_0c_2r_2 + \angle a_0c_2b_2 \geq (90° - \varepsilon) + 90° = 180° - \varepsilon$. Since $\varepsilon < 22.5°$, this contradicts Lemma 8(iii).

Now let b_2 lie to the right of $\text{ray}(r_2, c_2)$. Recall that every self-approaching b_2c_1-path must use c_2, so it is $\angle c_1c_2b_2 \geq 90°$. Therefore, b_2 cannot lie inside the counterclockwise angle between c_2r_2 and c_2c_1, since it is $\angle_{\text{ccw}}(\overrightarrow{c_2r_2}, \overrightarrow{c_2c_1}) \leq 90° + \varepsilon < \angle r_2c_2b_2 + \angle b_2c_2c_1$. Thus, b_2 is above c_2c_1, and it is $\angle r_2c_2b_2 = \angle c_1c_2r_2 + \angle c_1c_2b_2 \geq (90° - \varepsilon) + 90° = 180° - \varepsilon$. Again, since $\varepsilon < 22.5°$, this contradicts Lemma 8(iii). It follows $\angle r_2a_2b_2 \geq 90°$.

Analogously, we prove $\angle r_2c_2b_2 \geq 90°$. Thus, by Lemma 8(iii), $\angle r_2a_2b_2$, $\angle r_2c_2b_2 \in [90°, 90° + \varepsilon]$. Since $\angle a_2b_2c_2 \geq 90°$ by Lemma 8(i), b_2 lies to the right of $\text{ray}(r_2, a_2)$ and to the left of $\text{ray}(r_2, c_2)$. (If b_2 lies to the left of both rays, it is $\angle a_2b_2c_2 = \angle(\overrightarrow{a_2b_2}, \overrightarrow{c_2b_2}) \leq 2\varepsilon < 90°$.)

(ii) Similarly, if a self-approaching b_2a_0-path uses c_2 instead of a_2, it is $\angle r_2c_2b_2 \geq 180° - \varepsilon$. The last part follows analogously. □

The next lemma allows us to show that certain blocks are drawn smaller than their ancestors.

Lemma 10. *It holds:*

(i) $\frac{|ra|}{|rc|}, \frac{|rc|}{|ra|} \geq \cos\varepsilon$;

(ii) $\frac{|ac|}{|ra|}, \frac{|ac|}{|rc|} \leq \tan\varepsilon$;

(iii) *The distance from a to the line through rc is at least $|ac|\cos\varepsilon$.*

(iv) *Consider block μ containing a, b, c, r, vertex $u \neq a$ in G^a and $v \neq c$ in G^c,* $\deg(u) = \deg(v) = 4$. *Then,* $\frac{|au|}{|ac|} \leq \tan\varepsilon$, $\frac{|cv|}{|ac|} \leq \tan\varepsilon$, *and* $|uv| \leq (1 + 2\tan\varepsilon)|ac|$.

Proof. (i) Due to symmetry, we show only one part. By Lemma 8(iv), $\angle acr \in [90° - \varepsilon, 90° + \varepsilon]$. Therefore,

$$\frac{|ra|}{|rc|} = \frac{\sin\angle acr}{\sin\angle rac} \geq \frac{\sin(90° - \varepsilon)}{1} = \cos\varepsilon.$$

(ii) It is $\angle arc \leq \varepsilon$. Therefore,

$$\frac{|ac|}{|ra|} = \frac{\sin \angle arc}{\sin \angle acr} \leq \frac{\sin(\varepsilon)}{\sin(90^\circ - \varepsilon)} = \tan \varepsilon.$$

(iii) Let d be the point on the line through rc minimizing $|ad|$. Since $\angle acr \in [90^\circ - \varepsilon, 90^\circ + \varepsilon]$, it is $\angle(\overrightarrow{ac}, \overrightarrow{ad}) \leq \varepsilon$. Thus, $|ad| \geq |ac| \cos \varepsilon$.

(iv) By Lemma 8(iv), $\angle acu \leq \varepsilon$ and $\angle auc \in [90^\circ - \varepsilon, 90^\circ + \varepsilon]$. Thus,

$$\frac{|au|}{|ac|} = \frac{\sin \angle acu}{\sin \angle auc} \leq \frac{\sin \varepsilon}{\sin(90^\circ - \varepsilon)} = \tan \varepsilon.$$

Similarly, $|vc| \leq |ac| \tan \varepsilon$. Thus, it is $|uv| \leq |ua| + |ac| + |cv| \leq (1 + 2 \tan \varepsilon)|ac|$. □

From now on, let μ_0 be the root block of $G^{\bar{r}}$ and μ_1, μ_2, μ_3 its descendants such that $r(\mu_1) = c_0$, $r(\mu_2) = a_1$, $r(\mu_3) \in \{a_2, c_2\}$; see Fig. 7c. Light gray blocks are the subject of Lemma 11(i), which shows that several ancestor roots lie inside a cone with a small angle. Dark gray blocks are the subject of Lemma 11(ii), which considers the intersection of the cones corresponding to a pair of sibling blocks and shows that some of their ancestor roots lie inside a narrow strip; see Fig. 8a for a sketch.

Lemma 11. *Let μ be a block in G^{c_2} with vertices a, b, c, $r(\mu)$.*

(i) *Let μ have depth 5 in $G^{\bar{r}}$. Then, the cone $l^+_{ba} \cap l^+_{bc}$ contains $r(\mu)$, $r(\pi(\mu))$, $r(\pi^2(\mu))$ and $r(\pi^3(\mu))$.*

(ii) *Let μ have depth 4 in $G^{\bar{r}}$. There exist u in G^a and v in G^c of degree 4 and a strip S containing $r(\mu)$, $r(\pi(\mu))$, $r(\pi^2(\mu)) = r(\mu_2)$, such that u and v lie on the different boundaries of S, and it holds: $|uv| \leq (1 + 2 \tan \varepsilon)(\tan \varepsilon) \min\{|r(\mu)a|, |r(\mu)c|\}$.*

Proof. (i) Consider a self-approaching bb_0-path ρ_0 and a self-approaching bb_1-path ρ_1. By Lemma 9(ii) applied to μ, ba is the first edge of ρ_0 and bc the first edge of ρ_1. Since the cutvertices $r(\mu)$, $r(\pi(\mu))$, $r(\pi^2(\mu))$, $r(\pi^3(\mu))$ are on both ρ_0 and ρ_1, the statement holds.

(ii) Consider blocks μ_l, μ_r, such that $r(\mu_l) = a$ and $r(\mu_r) = c$. By (i), $r(\mu)$, $r(\pi(\mu))$, $r(\pi^2(\mu))$ are in $\Lambda := l^+_{b_l a_l} \cap l^+_{b_l c_l} \cap l^+_{b_r a_r} \cap l^+_{b_r c_r}$. Let $\vec{v_l}$ be the vector $\overrightarrow{b_l c_l}$ rotated by 90° clockwise and $\vec{v_r}$ be the vector $\overrightarrow{b_r a_r}$ rotated by 90° counterclockwise. Note that by Lemma 8(ii), G^{c_l}, G^{a_r} lie in $l^+_{b_l c_l}$, $l^+_{b_r a_r}$ respectively. Therefore, $\text{ray}(c_l, \vec{v_l})$ and $\text{ray}(a_r, \vec{v_r})$ (green resp. blue arrows in Fig. 8a) converge, since the converse would contradict Lemma 2. Let p be their intersection. Due to the chosen directions, $r(\mu)$, $r(\pi(\mu))$, $r(\pi^2(\mu))$ are below both c_l and a_r. Therefore, $r(\mu)$, $r(\pi(\mu))$, $r(\pi^2(\mu))$ are contained in the triangle $c_l a_r p$, which lies inside a strip S of width at most $|c_l a_r|$, whose respective boundaries contain c_l and a_r. By Lemma 10(iv) and (ii), $|c_l a_r| \leq (1 + 2 \tan \varepsilon)|ac| \leq (1 + 2 \tan \varepsilon)(\tan \varepsilon) \min\{|r(\mu)a|, |r(\mu)c|\}$. □

Again, we consider two siblings and the intersection of their corresponding strips, which forms a small diamond containing the root of the ancestor block; see Fig. 8b, 8c.

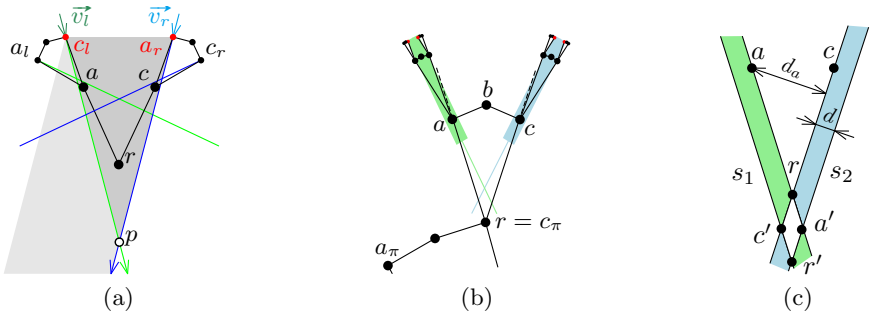

Figure 8: Showing the contradiction in Theorem 4.

Lemma 12. *Consider block μ_3 containing $r = r(\mu_3), a, b, c$, and let $r_\pi := r(\pi(\mu_3))$. It holds:* (i) $|r_\pi r| \leq \frac{(1+2\tan\varepsilon)(\tan\varepsilon)^2}{\cos\varepsilon}(|ra| + |rc|)$; (ii) $|ra|, |rc| \leq |rr_\pi|(\tan\varepsilon)^2$.

Proof. (i) Define $d = (1 + 2\tan\varepsilon)(\tan\varepsilon)^2|ac|$. Then, by Lemma 10(ii) and (iv) and Lemma 11(ii), vertices a, r and r_π are contained in a strip s_1 (green in Fig. 8b) of width at most d. Additionally, both boundaries of s_1 contain vertices of G^a (red dots), which lie in l^+_{ba} and, by Lemma 9(i), to the left of ray(r, a). Thus, the downward direction along s_1 is counterclockwise compared to $\vec{ar}$. (Otherwise, the green strip could not contain a.) Similarly, vertices c, r and r_0 are contained in a strip s_2 (blue) of width at most d, and both boundaries of s_2 contain vertices of G^c, which lie to the right of ray(r, c). Thus, the downward direction along s_2 is clockwise compared to $\vec{cr}$; see Fig. 8b.

Let us find an upper bound for the diameter of the parallelogram $s_1 \cap s_2$. In the critical case, the right side of s_1 touches ra, the left side of s_2 touches rc, and the width of both strips is d; see Fig. 8c. Let a' (resp. c') be the intersection of the right (resp. left) sides of s_1 and s_2, and r' the intersection of the left side of s_1 and right side of s_2. Let d_a be the distance from a to the line through rc and d_c the distance from c to the line through ra. By Lemma 10(iii), it is $d_a, d_c \geq |ac|\cos\varepsilon$. Moreover, it holds: $\frac{|ra'|}{|ra|} = \frac{d}{d_a}$ and $\frac{|rc'|}{|rc|} = \frac{d}{d_c}$. Therefore, $|ra'| \leq \frac{d|ra|}{|ac|\cos\varepsilon}$, $|rc'| \leq \frac{d|rc|}{|ac|\cos\varepsilon}$ and

$$|rr'| \leq |ra'| + |rc'| \leq \frac{(1+2\tan\varepsilon)(\tan\varepsilon)^2}{\cos\varepsilon}(|ra| + |rc|).$$

Since $\angle a'rc' \leq \varepsilon$, rr' is the diameter, thus, $|rr_\pi| \leq |rr'|$.

(ii) Let a_π and c_π be the two neighbors of r_π in the block $\mu_2 = \pi(\mu_3)$. It is $r \in \{a_\pi, c_\pi\}$. Assume $r = c_\pi$ as in Fig. 8b. By Lemma 10(iv), it is $\frac{|ac_\pi|}{|a_\pi c_\pi|} \leq \tan\varepsilon$. By Lemma 10(ii), it is $\frac{|a_\pi c_\pi|}{|r_\pi c_\pi|} \leq \tan\varepsilon$. It follows: $|ra| = |ac_\pi| \leq |r_\pi c_\pi|(\tan\varepsilon)^2 = |rr_\pi|(\tan\varepsilon)^2$. Analogously, $|rc| \leq |rr_\pi|(\tan\varepsilon)^2$. □

For $\varepsilon \leq 22.5°$, the two claims of Lemma 12 contradict each other. This concludes the proof of Theorem 4.

4 Planar Increasing-Chord Drawings of 3-Trees

In this section, we show how to construct planar increasing-chord drawings of planar 3-trees. We make use of *Schnyder labelings* [24] and drawings of triangulations based on them. For a plane triangulation $G = (V, E)$ with external vertices r, g, b, its Schnyder labeling is an orientation and partition of the interior edges into three trees T_r, T_g, T_b (called *red*, *green* and *blue tree*), such that for each internal vertex v, its incident edges appear in the following clockwise order: exactly one outgoing red, an arbitrary number of incoming blue, exactly one outgoing green, an arbitrary number of incoming red, exactly one outgoing blue, an arbitrary number of incoming green. Each of the three outer vertices r, g, b serves as the root of the tree in the same color and all its incident interior edges are incoming in the respective color. For $v \in V$, let R_v^r (the *red region* of v) denote the region bounded by the vg-path in T_g, the vb-path in T_b and the edge gb. Let $|R_v^r|$ denote the number of the interior faces in R_v^r. The green and blue regions R_v^g, R_v^b are defined analogously. Assigning v the coordinates $(|R_v^r|, |R_v^g|, |R_v^b|) \in \mathbb{R}^3$ results in a plane straight-line drawing of G in the plane $\{x = (x_1, x_2, x_3) \mid x_1 + x_2 + x_3 = f - 1\}$ called *Schnyder drawing*. Here, f denotes the number of faces of G. For a thorough introduction to this topic, see the book of Felsner [10].

For $\alpha, \beta \in [0°, 360°]$, let $[\alpha, \beta]$ denote the corresponding counterclockwise cone of directions. We consider drawings satisfying the following constraints.

Definition 1. *Let $G = (V, E)$ be a plane triangulated graph with a Schnyder labeling. For $0° \leq \alpha \leq 60°$, we call an arbitrary planar straight-line drawing of G* α-Schnyder *if for each internal vertex $v \in V$, its outgoing red edge has direction in $[90° - \frac{\alpha}{2}, 90° + \frac{\alpha}{2}]$, blue in $[210° - \frac{\alpha}{2}, 210° + \frac{\alpha}{2}]$ and green in $[330° - \frac{\alpha}{2}, 330° + \frac{\alpha}{2}]$ (see Fig. 9a).*

According to Definition 1, classical Schnyder drawings are 60°-Schnyder; see, e.g., Lemma 4 in [8]. The next lemma shows an interesting connection between α-Schnyder and increasing-chord drawings.

Lemma 13. *For any $\alpha \leq 30°$, α-Schnyder drawings are increasing-chord drawings.*

Proof. Let $G = (V, E)$ be a plane triangulation with a given Schnyder labeling and Γ a corresponding 30°-Schnyder drawing. Let r, g, b be the red, green and blue external vertex, respectively, and T_r, T_g, T_b the directed trees of the corresponding color.

Consider vertices $s, t \in V$. First, note that monochromatic directed paths in Γ have increasing chords by Lemma 1. Assume s and t are not connected by such a path. Then, they are both internal and s is contained in one of the regions R_t^r, R_t^g, R_t^b. Without loss of generality, we assume $s \in R_t^r$. The sr-path in T_r crosses the boundary of R_t^r, and we assume without loss of generality that it crosses the blue boundary of R_t^r in $u \neq t$; see Fig. 9b. The other cases are symmetric.

Let ρ_r be the su-path in T_r and ρ_b the tu-path in T_b; see Fig. 9c. On the one hand, the direction of a line orthogonal to a segment of ρ_r is in $[345°, 15°] \cup [165°, 195°]$. On the other hand, ρ_b is contained in a cone $[15°, 45°]$ with apex u. Thus, $\rho_b^{-1} \subseteq \text{front}(\rho_r)$, and $\rho_r.\rho_b^{-1}$ is self-approaching by Fact 2. By a symmetric argument it is also self-approaching in the other direction, and hence has increasing chords. □

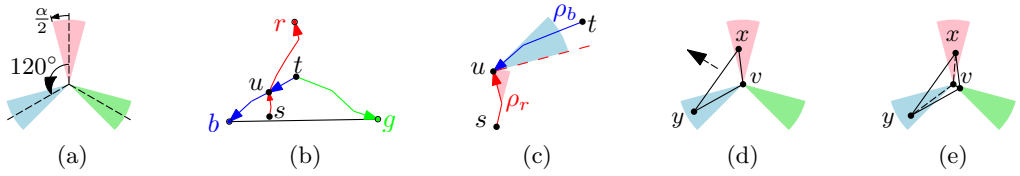

(a) (b) (c) (d) (e)

Figure 9: (a)–(c) 30°-Schnyder drawings are increasing-chord; (d),(e) special case of planar 3-trees.

Planar 3-trees are the graphs obtained from a triangle by repeatedly choosing a (triangular) face f, inserting a new vertex v into f, and connecting v to each vertex of f.

Lemma 14. *Planar 3-trees have α-Schnyder drawings for any $0° < \alpha \leq 60°$.*

Proof. We describe a recursive construction of an α-Schnyder drawing of a planar 3-tree. We use the pattern in Fig. 9a consisting of three cones with angle $0° < \alpha \leq 60°$ to maintain the following invariant.

For each inner face f, the pattern can be centered at a point p in the interior of f, such that every cone of the pattern contains one vertex of f in its interior.

We start with an equilateral triangle. Obviously, the invariant holds for the single inner face f by choosing p to be the barycenter of f.

Assume the invariant holds for each inner face of the drawing created so far. We prove that the invariant can be maintained after adding a new vertex. Consider an inner face f with corners x, y, z. We move the pattern from Fig. 9a, such that its center lies in the interior point p of f from the invariant. Without loss of generality, let x be in the red cone of the pattern, y in the blue cone and z in the green. We insert the new vertex v at point p and connect v to x, y, z. We make the edge vx outgoing red, vy outgoing blue and vz outgoing green.

We now show that the invariant holds for the three newly created faces $f_1 = xyv$, $f_2 = yzv$ and $f_3 = zxv$. Consider f_1 first. If we place the pattern at v, by the invariant for face f, one cone of the pattern contains x and another contains y in its interior; see Fig. 9d. It is now possible to move the pattern inside the triangle xyv slightly, such that v is in the interior of the third cone; see Fig. 9e. This proves the invariant for f_1, and the proof for f_2 and f_3 is analogous. □

Lemmas 13 and 14 provide a constructive proof for the following theorem.

Theorem 5. *Every planar 3-tree has a planar increasing-chord drawing.*

5 Self-Approaching Drawings in the Hyperbolic Plane

Kleinberg [15] showed that every tree can be drawn greedily in the hyperbolic plane $\mathbb{H}^2$. This is not the case in $\mathbb{R}^2$. Thus, $\mathbb{H}^2$ is more powerful than $\mathbb{R}^2$ in this regard. Since

self-approaching drawings are closely related to greedy drawings, it is natural to investigate the existence of self-approaching drawings in $\mathbb{H}^2$.

We shall use the *Poincaré disk* model for $\mathbb{H}^2$, in which $\mathbb{H}^2$ is represented by the unit disk $D = \{x \in \mathbb{R}^2 : |x| < 1\}$ and the geodesics are represented by arcs of circles orthogonal to the boundary of D. We consider a drawing of a graph in $\mathbb{H}^2$ straight-line, if the edges are drawn as arcs of such circles. For an introduction to the Poincaré disk model, see, for example, Kleinberg [15] and the references therein.

First, let us consider a tree $T = (V, E)$. A drawing of T in $\mathbb{R}^2$ is self-approaching if and only if no normal on an edge of T in any point crosses another edge [1]. The same condition holds in $\mathbb{H}^2$.

Lemma 15. *A straight-line drawing Γ of a tree T in $\mathbb{H}^2$ is self-approaching if and only if no normal on an edge of T crosses Γ in another point.*

Proof. The proof is similar to the Euclidean case. We present it for the sake of completeness. First, let Γ be a self-approaching drawing, for which the condition of the lemma is violated. Without loss of generality, let $\rho = (s, u, \ldots, t)$ be the st-path in T, such that the normal on su in a point r crosses ρ in another point. Due to the piecewise linearity of ρ, we may assume r to be in the interior of su. Let $H_+ = \{p = (p_x, p_y) \in D \mid p_y > 0\}$ and $H_- = \{p = (p_x, p_y) \in D \mid p_y < 0\}$ the top and bottom hemispheres of D. For $p_1, p_2 \in D$, let $d(p_1, p_2)$ denote the hyperbolic distance between p_1 and p_2, i.e., the hyperbolic length of the corresponding geodesics. We recall the following basic fact whose proof is given, e.g., by Kleinberg [15].

Claim 1. *Let $0 < y < 1$, $p_- = (0, -y)$, $p_+ = (0, y)$. Then, for each $p \in H_-$, it is $d(p, p_-) < d(p, p_+)$.*

Due to isometries, we can assume that r is in the origin of D, su is vertical, $s \in H_-$, $u \in H_+$. Let $a \in H_-$, $b \in H_+$ be two points on su, such that $|ar| = |rb|$. Since the normal on su in r crosses ρ, there must exist a point c on ρ, $c \in H_-$, such that a, b, c are on ρ in this order. However, it is $d(a, c) < d(b, c)$, a contradiction to ρ being self-approaching.

Let Γ be a drawing of T, for which the condition holds. Let a, b, c be three consecutive points on a path ρ in Γ. First, assume a, b lie on the same arc of Γ. We apply an isometry to Γ, such that ab is vertical, $a \in H_-$, $b \in H_+$, and a, b are equidistant from the origin o. The normal to ρ in o is the equator. Thus, it is $c \notin H_-$, and $d(b, c) \leq d(a, c)$. By applying this argument iteratively, this inequality also holds if a, b lie on different arcs. □

According to the characterization by Alamdari et al. [1], some binary trees have no self-approaching drawings in $\mathbb{R}^2$. We show that this is no longer the case in $\mathbb{H}^2$.

Theorem 6. *Let $T = (V, E)$ be a tree, such that each node of T has degree either 1 or 3. Then, T has a self-approaching drawing in $\mathbb{H}^2$, in which every arc has the same hyperbolic length and every pair of incident arcs forms an angle of* 120°.

Proof. For convenience, we subdivide each edge of T once. We shall show that both pieces are collinear in the resulting drawing Γ and have the same hyperbolic length.

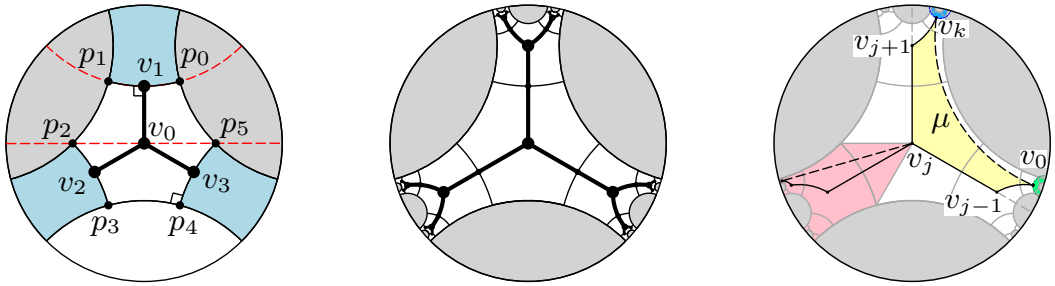

(a) (b) (c)

Figure 10: Constructing increasing-chord drawings of binary trees and cactuses in $\mathbb{H}^2$.

First, consider a regular hexagon $\hexagon = p_0p_1p_2p_3p_4p_5$ centered at the origin o of D; see Fig. 10a. In $\mathbb{H}^2$, it can have angles smaller than 120°. We choose them to be 90° (any angle between 0° and 90° would work). Next, we draw a $K_{1,3}$ with center v_0 in o and the leaves v_1, v_2, v_3 in the middle of the arcs p_0p_1, p_2p_3, p_4p_5 respectively.

For each such building block of the drawing consisting of a $K_{1,3}$ inside a regular hexagon with 90° angles, we add its copy mirrored at an arc of the hexagon containing a leaf node of the tree constructed so far. For example, in the first iteration, we add three copies of $\hexagon$ mirrored at p_0p_1, p_2p_3 and p_4p_5, respectively, and the corresponding inscribed $K_{1,3}$ subtrees. The construction after two iterations is shown in Fig. 10b. This process can be continued infinitely to construct a drawing Γ_∞ of the infinite binary tree. However, we stop after we have completed Γ for the tree T.

We now show that Γ_∞ (and thus also Γ) has the desired properties. Due to isometries and Lemma 15, it suffices to consider edge $e = v_0v_1$ and show that a normal on e does not cross Γ_∞ in another point. To see this, consider Fig. 10a. Due to the choice of the angles of $\hexagon$, all the other hexagonal tiles of Γ_∞ are contained in one of the three blue quadrangular regions $\square_i := l^+_{v_0v_i} \setminus (l^+_{v_ip_{2i-1}} \cup l^+_{v_ip_{2i-2}})$, $i = 1, 2, 3$. Thus, the regions $l^+_{v_1p_1}$ and $l^+_{v_1p_0}$ (gray) contain no point of Γ_∞. Therefore, since each normal on v_0v_1 is contained in the "slab" $D \setminus (l^+_{v_0v_1} \cup l^+_{v_1v_0})$ bounded by the diameter through p_2, p_5 and the line through p_0, p_1 (dashed) and is parallel to both of these lines, it contains no other point of Γ_∞. □

We note that our proof is similar in spirit to the one by Kleinberg [15], who also used tilings of $\mathbb{H}^2$ to prove that any tree has a greedy drawing in $\mathbb{H}^2$.

As in the Euclidean case, it can be easily shown that if a tree T contains a node v of degree 4, it has a self-approaching drawing in $\mathbb{H}^2$ if and only if T is a subdivision of $K_{1,4}$ (apply an isometry, such that v is in the origin of D). This completely characterizes the trees admitting a self-approaching drawing in $\mathbb{H}^2$. Further, it is known that every binary cactus and, therefore, every 3-connected planar graph has a binary spanning tree [5, 17].

Corollary 2. (i) *A tree T has an increasing-chord drawing in $\mathbb{H}^2$ if and only if T either has maximum degree 3 or is a subdivision of $K_{1,4}$.*

(ii) *Every binary cactus and, therefore, every 3-connected planar graph has an increasing-chord drawing in $\mathbb{H}^2$.*

Again, note that this is not the case for binary cactuses in $\mathbb{R}^2$; see the example in Theorem 4. We use the above construction to produce *planar* self-approaching drawings of binary cactuses in $\mathbb{H}^2$. We show how to choose a spanning tree and angles at vertices of degree 2, such that non-tree edges can be added without introducing crossings; see Fig. 10c for a sketch.

Corollary 3. *Every binary cactus has a planar increasing-chord drawing in* $\mathbb{H}^2$.

Proof. Without loss of generality, let G be a binary cactus rooted at block ν such that each block μ of G is either a single edge or a cycle. For each block μ forming a cycle $r(\mu) = v_0, v_1, \ldots, v_k, v_0$, we remove edge v_0v_k, thus obtaining a binary tree T. We embed it similarly to the proof of Theorem 6 such that additionally the counterclockwise angle $\angle v_{j-1}v_jv_{j+1} = 120°$ for $j = 1, \ldots, k-1$. Obviously, T is drawn in a planar way since for each edge e of T, each half of e is drawn inside its hexagon.

It remains to show that for each μ, adding arc v_0v_k introduces no crossings. For each $j = 1, \ldots, k-1$, we can apply an isometry to the drawing, such that v_j is in the origin and $\overrightarrow{v_jv_{j+1}}$ points upwards; see Fig. 10c. According to the construction of T, subcactus $G_\mu^{v_0}$ (maximal subcactus of G containing v_0 and no other vertex of μ) lies in the green region contained in $l^+_{v_1v_0}$ and $G_\mu^{v_k}$ in the blue region contained in $l^+_{v_{k-1}v_k}$. Since $v_0 \notin l^+_{v_{k-1}v_k}$ and $v_k \notin l^+_{v_1v_0}$, arc v_0v_k crosses neither $G_\mu^{v_0}$ nor $G_\mu^{v_k}$. Furthermore, v_0 and v_k lie inside the 120° cone Λ_j formed by $\mathrm{ray}(v_j, v_{j+1})$ and $\mathrm{ray}(v_j, v_{j-1})$. Thus, v_0v_k does not cross $v_{j-1}v_j$, v_jv_{j+1}. Since subcactus $G_\mu^{v_j}$ is in $\mathbb{H}^2 \setminus \Lambda_j$ (it lies in the red area in Fig. 10c), it is not crossed by v_0v_k either. □

6 Conclusion

We have studied the problem of constructing self-approaching and increasing-chord drawings of 3-connected planar graphs and triangulations in the Euclidean and hyperbolic plane. Due to the fact that every such graph has a spanning binary cactus, and in the case of a triangulation even one that has a special type of triangulation (downward-triangulation), self-approaching and increasing-chord drawings of binary cactuses played an important role.

We showed that, in the Euclidean plane, downward-triangulated binary cactuses admit planar increasing-chord drawings, and that the condition of being downward-triangulated is essential as there exist binary cactuses that do not admit a (not necessarily planar) self-approaching drawing. Naturally, these results imply the existence of non-planar increasing-chord drawings of triangulations. It remains open whether every 3-connected planar graph has a self-approaching or increasing-chord drawing. If this is the case, according to our example in Theorem 4, the construction must be significantly different from both known proofs [5, 17] of the weak Papadimitriou-Ratajczak conjecture [20] (you cannot just take an arbitrary spanning binary cactus) and would prove a stronger statement.

For planar 3-trees, which are special triangulations, we introduced α-Schnyder drawings, which have increasing chords for $\alpha \leq 30°$, to show the existence of planar increasing-chord drawings. It is an open question whether this method works for further

classes of triangulations. Which triangulations admit α-Schnyder drawings for arbitrarily small values of α or for $\alpha = 30°$?

Finally, we studied drawings in the hyperbolic plane. Here we gave a complete characterization of the trees that admit an increasing-chord drawing (which then is planar) and used it to show the existence of non-planar increasing-chord drawings of 3-connected planar graphs. For binary cactuses even a planar increasing-chord drawing exists.

It is worth noting that all self-approaching drawings we constructed are actually increasing-chord drawings. Is there a class of graphs that admits a self-approaching drawing but no increasing-chord drawing?

References

[1] Alamdari, S., Chan, T.M., Grant, E., Lubiw, A., Pathak, V.: Self-approaching graphs. In: W. Didimo, M. Patrignani (eds.) Graph Drawing (GD'12), *LNCS*, vol. 7704, pp. 260–271. Springer (2013). doi:10.1007/978-3-642-36763-2_23

[2] Angelini, P., Colasante, E., Di Battista, G., Frati, F., Patrignani, M.: Monotone drawings of graphs. J. Graph Algorithms Appl. **16**(1), 5–35 (2012). doi:10.7155/jgaa.00249

[3] Angelini, P., Di Battista, G., Frati, F.: Succinct greedy drawings do not always exist. Networks **59**(3), 267–274 (2012). doi:10.1002/net.21449

[4] Angelini, P., Didimo, W., Kobourov, S., Mchedlidze, T., Roselli, V., Symvonis, A., Wismath, S.: Monotone drawings of graphs with fixed embedding. Algorithmica **71**(2), 233–257 (2013). doi:10.1007/s00453-013-9790-3

[5] Angelini, P., Frati, F., Grilli, L.: An algorithm to construct greedy drawings of triangulations. J. Graph Algorithms Appl. **14**(1), 19–51 (2010). doi:10.7155/jgaa.00197

[6] Barnette, D.: Trees in polyhedral graphs. Canad. J. Math. **18**, 731–736 (1966)

[7] Dehkordi, H.R., Frati, F., Gudmundsson, J.: Increasing-chord graphs on point sets. J. Graph Algorithms Appl. **19**(2), 761–778 (2015). doi:10.7155/jgaa.00348

[8] Dhandapani, R.: Greedy drawings of triangulations. Discrete Comput. Geom. **43**(2), 375–392 (2010). doi:10.1007/s00454-009-9235-6

[9] Eppstein, D., Goodrich, M.T.: Succinct greedy geometric routing using hyperbolic geometry. IEEE Trans. Computers **60**(11), 1571–1580 (2011). doi:10.1109/TC.2010.257

[10] Felsner, S.: Geometric Graphs and Arrangements, chap. 2, pp. 17–42. Advanced Lectures in Mathematics. Vieweg+Teubner Verlag (2004). doi:10.1007/978-3-322-80303-0_2

[11] Goodrich, M.T., Strash, D.: Succinct greedy geometric routing in the Euclidean plane. In: Y. Dong, D.Z. Du, O. Ibarra (eds.) Algorithms and Computation (ISAAC'09), *LNCS*, vol. 5878, pp. 781–791. Springer (2009). doi:10.1007/978-3-642-10631-6_79

[12] Huang, W., Eades, P., Hong, S.H.: A graph reading behavior: Geodesic-path tendency. In: IEEE Pacific Visualization Symposium (PacificVis'09), pp. 137–144 (2009). doi:10.1109/PACIFICVIS.2009.4906848

[13] Icking, C., Klein, R., Langetepe, E.: Self-approaching curves. Math. Proc. Camb. Phil. Soc. **125**, 441–453 (1999). doi:10.1017/S0305004198003016

[14] Kindermann, P., Schulz, A., Spoerhase, J., Wolff, A.: On monotone drawings of trees. In: C. Duncan, A. Symvonis (eds.) Graph Drawing (GD'14), *LNCS*, vol. 8871, pp. 488–500. Springer (2014). doi:10.1007/978-3-662-45803-7_41

[15] Kleinberg, R.: Geographic routing using hyperbolic space. In: Computer Communications (INFOCOM'07), pp. 1902–1909 (2007). doi:10.1109/INFCOM.2007.221

[16] Lee, B., Plaisant, C., Parr, C.S., Fekete, J.D., Henry, N.: Task taxonomy for graph visualization. In: AVI Workshop on Beyond Time and Errors: Novel Evaluation Methods for Information Visualization (BELIV'06), pp. 1–5. ACM (2006). doi:10.1145/1168149.1168168

[17] Leighton, T., Moitra, A.: Some results on greedy embeddings in metric spaces. Discrete Comput. Geom. **44**(3), 686–705 (2010). doi:10.1007/s00454-009-9227-6

[18] Nöllenburg, M., Prutkin, R.: Euclidean greedy drawings of trees. In: H. Bodlaender, G. Italiano (eds.) European Symposium on Algorithms (ESA'13), *LNCS*, vol. 8125, pp. 767–778. Springer (2013). doi:10.1007/978-3-642-40450-4_65

[19] Nöllenburg, M., Prutkin, R., Rutter, I.: On self-approaching and increasing-chord drawings of 3-connected planar graphs. In: C.A. Duncan, A. Symvonis (eds.) Graph Drawing (GD'14), *LNCS*, vol. 8871, pp. 476–487. Springer Berlin Heidelberg (2014). doi:10.1007/978-3-662-45803-7_40

[20] Papadimitriou, C.H., Ratajczak, D.: On a conjecture related to geometric routing. Theoret. Comput. Sci. **344**(1), 3–14 (2005). doi:10.1016/j.tcs.2005.06.022

[21] Purchase, H.C., Hamer, J., Nöllenburg, M., Kobourov, S.G.: On the usability of Lombardi graph drawings. In: W. Didimo, M. Patrignani (eds.) Graph Drawing (GD'12), *LNCS*, vol. 7704, pp. 451–462. Springer (2013). doi:10.1007/978-3-642-36763-2_40

[22] Rao, A., Ratnasamy, S., Papadimitriou, C., Shenker, S., Stoica, I.: Geographic routing without location information. In: Mobile Computing and Networking (MobiCom'03), pp. 96–108. ACM (2003). doi:10.1145/938985.938996

[23] Rote, G.: Curves with increasing chords. Math. Proc. Camb. Phil. Soc. **115**, 1–12 (1994). doi:10.1017/S0305004100071875

[24] Schnyder, W.: Embedding planar graphs on the grid. In: ACM-SIAM Symposium on Discrete Algorithms (SODA'90), pp. 138–148. SIAM (1990)

[25] Wang, J.J., He, X.: Succinct strictly convex greedy drawing of 3-connected plane graphs. Theoret. Comput. Sci. **532**, 80–90 (2014). doi:10.1016/j.tcs.2013.05.024